INTERNATIONAL
HELLENIC
UNIVERSITY

Numerical Simulation of a flat plate collector

Thomas Tsirakoglou

SID: 3302100012

SCHOOL OF SCIENCE & TECHNOLOGY
A thesis submitted for the degree of
Master of Science (MSc) in Energy Systems

SEPTEMBER 2011
THESSALONIKI – GREECE

INTERNATIONAL
HELLENIC
UNIVERSITY

Numerical Simulation of a flat plate collector

Thomas Tsirakoglou

SID: 3302100012

Supervisor:	

SCHOOL OF SCIENCE & TECHNOLOGY
A thesis submitted for the degree of
Master of Science (MSc) in Energy Systems

SEPTEMBER 2011
THESSALONIKI – GREECE

DISCLAIMER

This dissertation is submitted in part candidacy for the degree of Master of Science in Energy Systems, from the School of Science and Technology of the International Hellenic University, Thessaloniki, Greece. The views expressed in the dissertation are those of the author entirely and no endorsement of these views is implied by the said University or its staff.

This work has not been submitted either in whole or in part, for any other degree at this or any other university.

Signed: ....

Name: Thomas Tsirakoglou..

Date: 26/9/2011..

Abstract

This dissertation was written as a part of the MSc in Energy Systems at the International Hellenic University. It deals with the analysis of the operation of flat plate solar collectors which leads to the numerical simulation of their performance.

Solar collectors are a widespread means of exploiting solar energy. They are special kinds of heat exchangers that transform solar radiation energy to internal energy of the transport medium. There are different kinds of solar collectors which can be distinguished by their concentration or not, the type of heat transfer liquid used, the temperature range of the working fluid, their and whether they are covered or uncovered.

The evaluation of collector performance requires the calculation of the absorbed solar radiation and the heat loss to the surroundings. The equations describing these variables are developed in detail in this dissertation and they constitute the model for the collector numerical simulation.

I would like to thank Dr. Georgios Martinopoulos for his concern and advice which helped me accomplish this dissertation.

Thomas Tsirakoglou
26/9/2011

Contents

1 Introduction

1.1 General aim of dissertation

The general aim of this dissertation is to model the performance of a flat plate solar collector using MATLAB which is a numerical computing environment and a fourth-generation programming language.

In order to achieve this goal, the operation and performance of the flat plate collector will be numerically simulated via several equations. The equations are an expression of the energy equilibrium of the collector, equating the solar gains minus losses with the thermal energy gained by the working fluid of the collector.

1.2 Solar energy

Energy from the sun in the form of solar radiation supports almost all life on earth via photosynthesis and drives the earth's climate and weather. Sunlight is the main source of energy to the surface of the earth that can be harnessed via a variety of natural and synthetic processes. Because solar energy is available as long as the sun is available, it is considered a renewable source of energy. It is a clean source of energy as well due to the fact that it does not produce any pollutants that could harm the environment.

There are a few types of ways in which solar energy can be harnessed like solar photovoltaic conversion, solar thermal energy and passive solar energy. Solar photovoltaic conversion is what is used to convert the sun's rays into electricity through the use of solar panels. The amount of solar energy generated depends on the amount of radiation the panels or solar cells receive. This is the most common of all solar energy utilisations. Solar thermal energy uses the sun's rays to heat dwellings and water instead of using oil or gas.

Solar thermal collectors collect heat energy which is then transferred to the working fluid in the heating or plumbing systems. This form of solar power use is relatively cheap and environmental-friendly. Passive solar energy is the heating of a home or building through architectural design. Structures or buildings are constructed in a way to capture the sun’s power through the use of windows or tanks. These systems heat dwellings or water without any need for a collector of any kind [1].

2 Solar thermal systems

2.1 History of exploitation of solar energy

The principles of solar heat have been known for thousands of years. A black surface gets hot in the sun, while a lighter coloured surface remains cooler. This principle is used by solar water collectors which are one of the best known applications for the direct use of the sun's energy. They were developed some two hundred years ago and the first known flat plate collector was made by Swiss scientist Horace de Saussure in 1767. Solar technology advanced to roughly its present design in 1908 when William J. Bailey of the Carnegie Steel Company invented a collector with an insulated box and copper coils. This collector was very similar to the thermosiphon system which is used nowadays [2].

Little interest was shown in such devices until the world-wide oil crisis of 1973. This crisis promoted new interest in alternative energy sources. As a result, solar energy has received increased attention and many countries have taken a keen interest in new developments of solar energy systems. The efficiency of solar heating systems and collectors has improved since the early 1970s mainly due to the use of low-iron, tempered glass for glazing, improved insulation and the development of durable selective coatings [3].

2.2 Measurement of solar radiation

In solar system design it is essential to know the amount of sunlight available at a particular location at a given time. The two most common methods which characterize solar radiation are solar radiance (or radiation) and solar insolation. Solar radiance is an instantaneous power density in units of kW/m^2 which is strongly dependent on location and local weather. Solar radiance measurements consist of global and direct radiation measurements taken periodically throughout the day. The measurements are taken using either a pyranometer (Figure 1), which measures global radiation, or a pyrheliometer (Figure 2), which measures direct radiation. In well established locations, this data has been collected for more than twenty years.

An alternative method of measuring solar radiation, which is less accurate but also less expensive, is using a sunshine recorder. These sunshine recorders measure the number of hours in the day during which the sunshine is above a certain level (typically 200mW/cm²). Data collected in this way can be used to determine the solar insolation by comparing the measured number of sunshine hours to those based on calculations and including several correction factors.

A method to estimate solar insolation is cloud-cover data taken from existing satellite images.

While solar radiance is most commonly measured, another form of radiation data used in system design is solar insolation. Solar insolation is the total amount of solar energy received at a particular location during a specified time period, often in units of kWh/(m² day). While the units of solar insolation and solar radiance are both a power density, solar insolation is quite different than solar radiance as solar insolation is the instantaneous solar radiance averaged over a given time period.

Solar radiation for a particular location can be given in several ways including:

- Typical mean year data for a particular location
- Average daily, monthly or yearly solar insolation for a given location
- Sunshine hours data
- Solar insolation based on satellite cloud cover data
- Calculations of solar radiation [4]

Figure 1: Pyranometer [5]

Figure 2: Pyrheliometer [6]

2.3 Solar thermal capacity in operation worldwide

The International Energy Agency's Solar Heating and Cooling Programme and major solar thermal trade associations have published new statistics on the use of solar thermal energy (Table 1). The solar thermal collector capacity in operation worldwide equalled 172.4 GW_{th} corresponding to 246.2 million square meters by the end of the year 2009. Of this, 151.5 GW_{th} were accounted for by flat plate and evacuated tube collectors and 19.7 GW_{th} for unglazed water collectors. Air collector capacity was installed to an extent of 1.2 GW_{th}. The vast majority of glazed and unglazed water and air collectors in operation are installed in China (101.5 GW_{th}), Europe (32.5 GW_{th}), the United States and Canada (15.0 GW_{th}), which together account for 86.4% of total installed capacity [7].

In the year 2009, a capacity of 36.5 GW_{th}, corresponding to 52.1 million square meters of solar collectors, was newly installed worldwide. This means an increase in collector installations of 25.3% compared to the year 2008. The main driver for the above average market growth in 2009 was China whereas in key European markets as well as in the United States and other important economic regions, such as in Japan, the solar thermal sector suffered from the economic downturn, resulting in stagnating or decreasing local markets [7].

The worldwide contribution of solar thermal installations to meeting the thermal energy demand for applications such as hot water or space heating has been greatly underestimated in the past. The underestimation of the capacity of solar thermal was due largely to the fact that solar thermal installations have traditionally been counted in square meters of collector area, a unit not comparable with other energy sources. Solar thermal experts agreed on a methodology to convert installed collector area into solar thermal capacity by using a factor of $0.7kW_{th}/m^2$ to derive the nominal capacity from the area of installed collectors [8].

The long-term technical potential for solar thermal energy, in terms of collector area in operation per capita, is higher in northern countries than in southern countries. The main reason is that in colder climates the demand for space heating is substantially higher and to produce the same amount of heat a larger collector area is needed.

In southern Europe there is a higher economical potential to use solar collectors for industrial process heat due to the higher radiation. The potential for solar cooling is also higher in southern Europe. However, these two factors cannot counterbalance the higher demand for space heating in cold climates. Table 2 shows the technical-economical potential for solar thermal energy in European Union, based on the average heat demand, solar radiation and on the population of each country.

Country	Water Collectors			TOTAL (MW_{th})
	unglazed	glazed	evacuated tube	
Australia	3,304	1,710.5	51.7	5,066.2
Austria	431.9	2,543.8	38.4	3,014.3
Brazil	890.3	2,799.7	-	3,690.0
China	-	7,105	94,395	101,500.0
Cyprus	-	598.2	2.7	601
France	74	1,279.1	23.4	1,376.4
Germany	504	7,508.7	844.5	8,880.7
Greece	-	2,852.2	1.8	2,853.9
India	-	1,987.3	169.6	2,168.3
Israel	20.6	2,827.5	-	2,848.5
Italy	30.6	1,263.2	177.1	1,470.9
Japan	-	3,936.1	68.1	4,334.8
Korea, South	-	1,047.6	-	1,047.6
Mexico	400.5	433.6	49.3	887.2
Spain	77.7	1,319.5	81.2	1,478.4
Switzerland	148.3	435.2	26.8	1,211.6
Taiwan	1.4	1,299.7	44.9	1,345.9
Turkey	-	8,424.5	-	8,424.5
United Kingdom	-	254.9	66.8	321.7
United States	12,455.5	1,787.8	61.4	14,373.2
TOTAL	19,703.9	54,915.5	96,539.1	172,368.6

Table 1: Total installed capacity in operation by the end of 2009 [7]

Country	Potential (per 1,000 Capita)	Potential (asolute)	Annual Energy Output	
	m^2	m^2	GWh	Mtoe
Austria	3,900	31,671,900	11,193	1
Belgium	3,900	40,021,800	16,827	1.4
Denmark	6,300	33,698,700	13,483	1.2
Finland	6,300	32,640,300	9,810	0.8
France	3,900	232,131,900	139,279	12
Germany	3,900	320,552,700	130,607	11.2
Greece	2,700	28,525,500	11,068	1
Ireland	3,900	14,898,000	6,704	0.6
Italy	3,300	190,885,200	116,543	10
Luxembourg	3,900	1,719,900	723	0.1
Netherlands	3,900	62,333,700	26,180	2.3
Portugal	2,700	27,062,100	16,237	1.4
Spain	2,700	106,623,000	64,448	5.5
Sweden	6,300	55,962,900	16,849	1.4
United Kingdom	3,900	233,309,700	102,196	8.8
TOTAL	3,740	1,412,037,300	682,149	58.7

Table 2: Technical-economical potential for solar thermal in EU [9]

3 Types of solar energy collectors

Solar energy collectors are special kinds of heat exchangers that transform solar radiation energy to internal energy of the transport medium. Solar collectors are the heart of most solar energy systems and can be used for nearly any process that requires heat. Specifically, they are used to warm buildings, heat water, generate electricity, dry crops or cook food. The solar collector is a device that absorbs part of the incoming solar radiation, converts it into heat and transfers the heat to a fluid (usually air, water or oil) flowing through the collector. The solar energy collected is carried from the circulating fluid either directly to the hot water or space conditioning equipment or to a thermal energy storage tank from which it can be drawn for use at night or on cloudy days.

There are basically two types of solar collectors: non-concentrating or stationary and concentrating. A non-concentrating collector has the same area for intercepting and absorbing solar radiation, whereas a sun-tracking concentrating solar collector (Figure 3) usually has concave reflecting surfaces to intercept and focus the sun's beam radiation to a smaller receiving area. Concentrating collectors are more suitable for high-temperature applications. Solar collectors can also be distinguished by the type of heat transfer fluid used (water, non-freezing liquid, air or heat transfer oil), the temperature range of the working fluid, their motion (stationary, single-axis tracking and two-axis tracking) and whether they are covered or uncovered (Figure 4). Stationary collectors are permanently fixed in position and do not track the sun.

The main characteristics and operation of the non-concentrating stationary solar collectors are described below.

There are two main types of collectors in this category: flat plate collectors (FPCs) and evacuated tube collectors (ETCs) [10].

Figure 3: Concentrating sun-tracking solar collector [11]

Figure 4: Unglazed solar collector [12]

3.1 Flat plate collectors

Flat plate collectors are the most common collectors for residential water-heating and space-heating installations. A typical flat plate collector is an insulated metal box with a glass or plastic cover called the glazing and a dark-coloured absorber plate. There are a few types of heat transfer fluid used in flat plate collectors like water, non-freezing liquid, air or heat transfer oil.

Solar radiation passes through the transparent cover and impinges on the blackened absorber surface of high absorptance, so a large portion of this energy is absorbed by the plate and transferred to the transport medium in the fluid tubes to be carried away for storage or use. The underside of the absorber plate and the two sides are well insulated to reduce conduction losses. The liquid tubes can be welded to the absorbing plate or they can be an integral part of the plate. They are connected at both ends by large-diameter header tubes. The most common designs for flat plate collectors are the header and riser collector and the serpentine design. The serpentine design collector does not present the potential problem of uneven flow distribution in the various riser tubes of the header and riser design, but serpentine collectors cannot work effectively in thermosiphon mode and need a pump to circulate the heat transfer fluid. The absorber plate can be a single sheet on which all risers are fixed or each riser can be fixed on a separate fin. The transparent cover of the collector reduces convection losses from the absorber plate and also reduces radiation losses.

The advantages of flat plate collectors are that they are not expensive to manufacture, they collect both beam and diffuse radiation and they are permanently fixed in position, so no tracking of the sun is required. In order to have the best possible performance, the collectors should be oriented directly towards the equator, facing south in the Northern Hemisphere and north in the Southern Hemisphere.

The main components of a flat plate collector (Figures 5, 6) are the following:

Cover: one ore more sheets of glass or other radiation-transmitting material.

Heat removal fluid passageways: tubes, fins or passages that conduct or direct the heat transfer fluid from the inlet tot the outlet.

Absorber plate: flat, corrugated or grooved plates to which the tubes, fins or passages are attached. The plate is usually coated with a high-absorptance, low-emittance layer.

Headers or manifolds: pipes and ducts to admit and discharge the fluid.

Insulation: used to minimize heat loss from the back and sides of the collector.

Container: the casing surrounds the aforementioned components and protects them from dust, moisture and any other material [10].

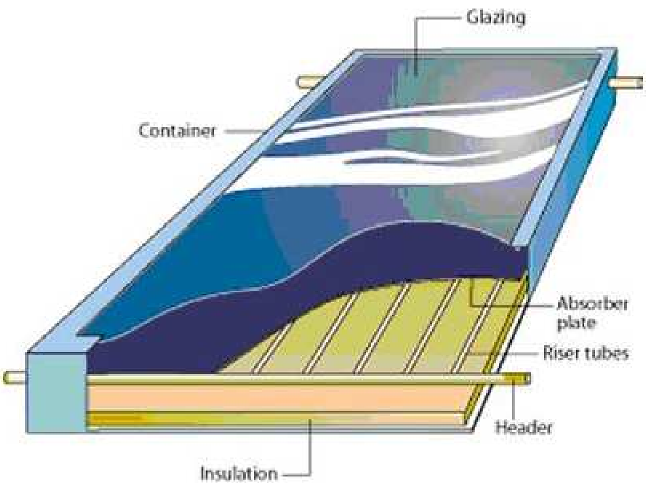

Figure 5: Flat plate collector [13]

Figure 6: Flat plate collector [14]

Liquid Collectors

In a liquid collector, solar energy heats a liquid as it flows through tubes in the absorber plate. For this type of collector, the flow tubes are attached to the absorber plate so the heat absorbed by the absorber plate is readily conducted to the liquid. The flow tubes can be routed in parallel or in a serpentine pattern. A serpentine pattern eliminates the possibility of header leaks and ensures uniform flow.

The simplest liquid systems use potable household water, which is heated as it passes directly through the collector and then flows to the house to be used for bathing, laundry, etc. This design is known as an open-loop or direct system. In areas where freezing temperatures are common, however, liquid collectors must either drain the water when the temperature drops or use an antifreeze type of heat-transfer fluid.

In systems with heat-transfer fluids, the transfer fluid absorbs heat from the collector and then passes through a heat exchanger. The heat exchanger, which generally is in the water storage tank inside the house, transfers heat to the water. Such designs are called closed-loop or indirect systems.

Air Collectors

Air collectors (Figure 7) have the advantage of eliminating the freezing and boiling problems associated with liquid systems. Although leaks are harder to detect and plug in an air system, they are also less troublesome than leaks in a liquid system. Air systems can often use less expensive materials, such as plastic glazing, because their operating temperatures are usually lower than those of liquid collectors.

Air collectors are simple, flat plate collectors used primarily for space heating and drying crops. The absorber plates in air collectors can be metal sheets, layers of screen, or non-metallic materials. The air flows through the absorber by natural convection or when forced by a fan. Because air conducts heat much less readily than liquid does, less heat is transferred between the air and the absorber than in a liquid collector. In some solar air-heating systems, fans on the absorber are used to increase air turbulence and improve heat transfer. The disadvantage of this strategy is that it can also increase the amount of power needed for fans and, thus, increase the costs of operating the system. In colder climates, the air is routed between the absorber plate and the back insulation to reduce heat loss through the glazing [15].

Figure 7: Hot air solar collector [16]

3.2 Evacuated tube collectors

Evacuated tube solar collectors (Figure 8) operate differently than the other collectors available on the market. These solar collectors consist of a heat pipe inside a vacuum-sealed tube. In an actual installation many tubes are connected to the same manifold.

Evacuated tube collectors combine a selective surface and an effective convection suppressor and this combination leads to good performance at high temperatures. The vacuum envelope reduces convection and conduction losses, so the collectors can operate at higher temperatures than flat plate collectors. Like flat plate collectors, they collect both direct and diffuse radiation. However, their efficiency is higher at low incidence angles.

Evacuated tube collectors use liquid-vapor phase change materials to transfer heat at high efficiency (Figure 9). These collectors consist of a heat pipe placed inside a vacuum-sealed tube. The pipe is then attached to a black copper fin that fills the tube and acts as the absorber plate. At the top of each tube there is a metal tip attached to a sealed pipe.

The heat pipe contains a small amount of fluid that undergoes an evaporating-condensing cycle. In this cycle, solar heat evaporates the liquid and the vapor ends up to the heat sink region where it condenses and releases its latent heat. The condensed fluid returns to the solar collector and the process is repeated. The released heat is picked up from the tubes by a liquid which flows through a heat exchanger. The heated liquid circulates through another heat exchanger and gives off its heat to a process or water stored in a solar storage tank. Another possibility is to use the evacuated tube collector connected directly to a hot water storage tank.

Because no evaporation or condensation above the phase-change temperature is possible, the heat pipe offers inherent protection from freezing and overheating. Evacuated tube collectors are produced in a variety of sizes, with outer diameters ranging from 30mm to about 100mm. The usual length of these collectors is about 2m [22, 23].

Figure 8: Evacuated tube collector [17]

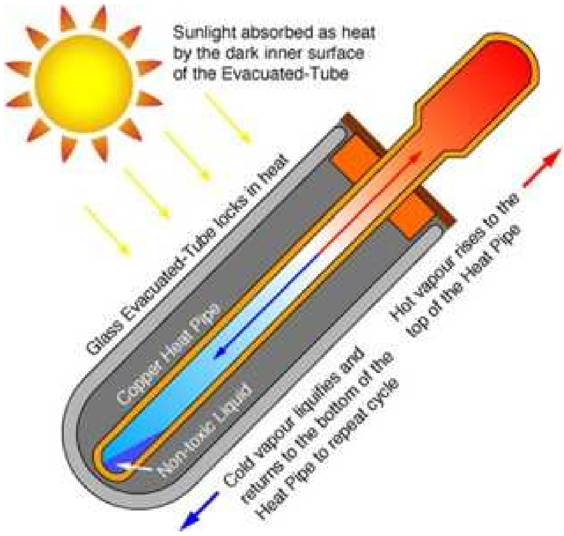

Figure 9: Evacuated tube cross section [18]

3.3 Materials used in flat plate collectors

Glazing materials

The most commonly used glazing material (Figure 10) in solar collectors is glass because it can transmit 90% of the incoming shortwave solar irradiation while transmitting none of the longwave radiation emitted outward by the absorber plate. Window glass usually has high iron content and is not suitable for use in solar collectors. Glass with low iron content has a relatively high transmittance for solar radiation but its transmittance is essentially zero for the longwave thermal radiation emitted by sun-heated surfaces.

Plastic films and sheets also possess high shortwave transmittance but they also have relatively high longwave transmittances as well. Additionally, plastics are generally limited in the temperatures they can sustain without deteriorating or undergoing dimensional changes. Only a few types of plastics can withstand the sun's ultraviolet radiation for long periods. However they are not broken by hail or stones and in the form of thin films they are completely flexible and have low mass.

Antireflective coatings and surface texture can improve transmission significantly. The effect of dirt and dust on collector glazing may be quite small and the cleansing effect of an occasional rainfall is usually adequate to maintain the transmittance within 2-4% of its maximum value. Dust is collected mostly during summertime when rainfall is less frequent, but due to the high magnitude of solar irradiation during this period the dust protects the collector from overheating [22, 23].

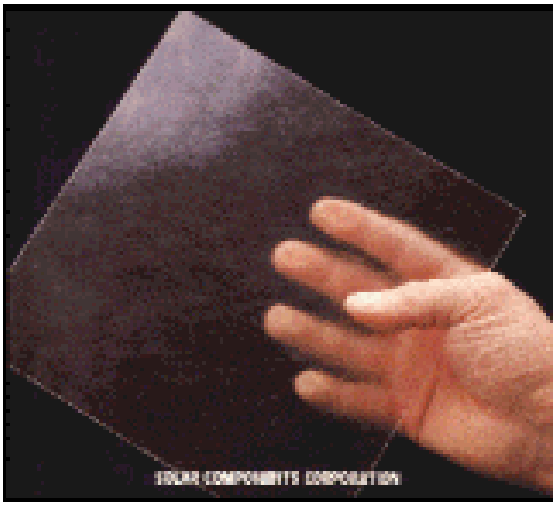

Figure 10: Glazing material [19]

Collector absorbing plates

The collector plate (Figure 11) absorbs as much of the irradiation as possible through the glazing while losing as little heat as possible upward to the atmosphere and downward through the back of the casing. The collector plates transfer the retained heat to the transport fluid. To maximize the energy collection, the absorber of a collector should have a coating that has high absorptance for solar radiation (short wavelength) and a low emittance for re-radiation (long wavelength). Such a surface is referred as a selective surface. The absorptance of the collector surface for shortwave solar radiation depends on the nature and colour of the coating and on the incident angle. Usually black colour is used.

Typical selective surfaces consist of a thin upper layer which is highly absorbent to shortwave solar radiation but relatively transparent to longwave thermal radiation, deposited on a surface that has a high reflectance and low emittance for longwave radiation. Selective surfaces are particularly important when the collector surface temperature is much higher than the ambient air temperature. The cheapest absorber coating is matte black paint. However, it is not selective and the performance of a collector produced in this way is low, especially for operating temperatures of more than 40°C above ambient. The most widely used type of selective coating is black chrome.

The materials most frequently used for collector plates are copper, aluminum and stainless steel. UV-resistant plastic extrusions are used for low-temperature applications. The back insulation of a flat plate collector is made from fiberglass or a mineral fiber mat that will not outgas at elevated temperatures.

The uncovered or unglazed solar collectors, usually called panel collectors, consist of a wide absorber sheet which is made of plastic and contains closed-space fluid passages. Materials used for plastic panel collectors include polypropylene, polyethylene, acrylic and polycarbonate [22].

Table 3 summarizes the materials used in each part of a solar thermal collector.

Figure 11: Absorber plate [20]

Part	Material
Absorber materials	Stainless steel or steel Aluminium or copper fins with stainless steel pipes Copper tubes extended to copper fins Copper tubes extended to aluminium fins
Absorber coating	Black paint Selective paint
Insulation	Rock wool or glass wool Polyurethane (non-CFC)
Glazing	Low iron tempered solar glass 3-5 mm Polymer
Casing	Aluminium Steel
Storage tank	Steel Stainless/galvanized steel Copper
Storage tank cover	Aluminium Galvanized steel

Table 3: Materials used for solar thermal collectors [21]

4 Simulation of flat plate collector

There are two different ways to evaluate the performance of a solar collector. The first one is to construct the collector and test it in actual conditions using the appropriate equipment. The second way is to develop a general model which would describe how all types of flat plate collector work. The simulation of collector performance through a model is much more cost-efficient than the construction and experimental testing of a collector. Consequently, the simulation model for plat collectors is a very useful tool for designing solar collectors.

A solar collector is a special kind of heat exchanger that uses solar radiation to heat the working fluid. Thus, the evaluation of collector performance requires the calculation of absorbed solar radiation and heat loss via certain equations. The equations describing the solar collector performance are developed in detail in this dissertation. Finally, these equations are used to develop the simulation model for flat plate collectors.

4.1 Solar radiation

First, some definitions concerning solar radiation are given. These definitions are useful in the process of the collector simulation [10, 22].

Beam radiation is the solar radiation received from the sun without having been scattered by the atmosphere. Beam radiation is often referred to as direct solar radiation.

Diffuse radiation is the solar radiation received from the sun after its direction has been changed by scattering by the atmosphere.

Total solar radiation is the sum of the beam and the diffuse solar radiation on a surface. The most common measurements of solar radiation are total radiation on a horizontal surface, often referred to as global radiation on the surface.

Solar time is the time based on the apparent angular motion of the sun across the sky, with solar noon the time the sun crosses the meridian of the observer. Solar time does not coincide with local clock time. The difference in minutes between solar time and standard time is:

$$\text{solar time} = \text{standard time} + 4 \times (L_{st} - L_{loc}) + E \quad (1)$$

where L_{st} is the standard meridian for the local time zone and L_{loc} is the longitude of the location in question. The equation of time E (in minutes) is determined from:

$$E = 229.2\,(0.000075 + 0.001868 \cos B - 0.032077 \sin B - \\ - 0.014615 \cos 2B - 0.04089 \sin 2B) \quad (2)$$

where

$$B = (n-1)\frac{360}{365} \quad (3)$$

and n is the day of the year.

The angles used in calculating solar radiation on the collector are also defined here.

Latitude φ is the angular location north or south of the equator, north positive;

$-90° \leq \varphi \leq 90°$

Declination δ is the angular position of the sun at solar noon (when the sun is on the local meridian) with respect to the plane of the equator, north positive;

$-23.45° \leq \delta \leq 23.45°$

Slope β is the angle between the plane of the surface in question and the horizontal; $0° \leq \beta \leq 180°$ ($\beta > 90°$ means that the surface has a downward facing component)

Surface azimuth angle γ is the deviation of the projection on a horizontal plane of the normal to the surface from the local meridian, with zero due south, east negative and west positive; $-180° \leq \gamma \leq 180°$

Hour angle ω is the angular displacement of the sun east or west of the local meridian due to rotation of the earth on its axis at 15° per hour, morning negative, afternoon positive.

Angle of incidence ϑ is the angle between the beam radiation on a surface and the normal to that surface.

Additional angles are defined that describe the position of the sun in the sky.

Zenith angle ϑ_z is the angle between the vertical and the line to the sun, in other words, the angle of incidence of beam radiation on a horizontal surface.

Solar altitude angle α_s is the angle between the horizontal and the line to the sun, i.e. the complement of the zenith angle.

Solar azimuth angle γ_s is the angular displacement from south of the projection of beam radiation on the horizontal plane. Displacements east of south are negative and west of south are positive.

The declination angle can be found from:

$$\delta = 23.45 \sin\left(360 \frac{284+n}{365}\right) \tag{4}$$

The angle of incidence of beam radiation on a surface is related to the other angles by:

$$\begin{aligned}\cos\theta = {} & \sin\delta\sin\phi\cos\beta - \sin\delta\cos\phi\sin\beta\cos\gamma + \cos\delta\cos\phi\cos\beta\cos\omega \\ & + \cos\delta\sin\phi\sin\beta\cos\gamma\cos\omega + \cos\delta\sin\beta\sin\gamma\sin\omega\end{aligned} \tag{5}$$

or:

$$\cos\theta = \cos(\phi-\beta)\cos\delta\cos\omega + \sin(\phi-\beta)\sin\delta \tag{6}$$

For horizontal surfaces:

$$\cos\theta_z = \cos\phi\cos\delta\cos\omega + \sin\phi\sin\delta \tag{7}$$

4.2 Physical model for flat plate solar collectors

The important parts of a liquid heating flat plate solar collector are the cover system with one or more glass or plastic covers, a plate for absorbing incident solar energy, parallel tubes attached to the plates and edge and back insulation. The detailed configuration may be different from one collector to the other; however, the basic geometry is similar for almost all flat plate collectors. The analysis of the flat plate solar collector in this chapter is performed based on the configuration shown in Figure 12.

Some assumptions made to model the flat plate solar collectors are the following [10, 22]:

1. The collector operates in steady state.

2. Construction is of sheet and parallel tube type.

3. The headers cover a small area of the collector and can be neglected.

4. The headers provide uniform flow to tubes.

5. There is one-dimensional heat flow through the back and side insulation and through the cover system.

6. There is a negligible temperature drop through a cover.

7. The covers are opaque to infrared radiation.

8. The sky can be considered as a blackbody for long-wavelength radiation at an equivalent sky temperature.

9. Temperature gradients around tubes can be neglected.

10. Temperature gradients in the direction of flow and between the tubes can be treated independently.

11. Loss through front and back are to the same ambient temperature.

12. Dust and dirt on the collector are negligible.

13. Shading of the collector absorber plate is negligible.

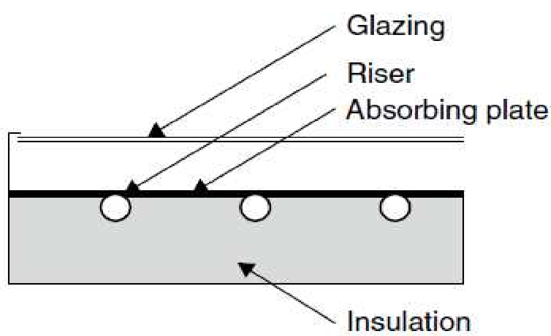

Figure 12: Cross section of a basic flat plate solar collector [10]

4.3 Energy balance equation

In steady state, the performance of a flat plate solar collector can be described by an energy balance equation that indicates the distribution of incident solar energy into useful energy gain, thermal losses and optical losses. The solar radiation absorbed by a collector per unit area of absorber S is equal to the difference between the incident solar radiation and the optical losses. The thermal energy loss from the collector to the surroundings can be represented as the product of a heat transfer coefficient U_L times the difference between the mean absorber plate temperature T_{pm} and the ambient temperature T_α. In steady state, the useful energy output of a collector is the difference between the absorbed solar radiation and the thermal loss [10, 22]:

$$Q_u = \left[A_p S - A_c U_L \left(T_{pm} - T_\alpha\right)\right]^+ \tag{8}$$

where A_c and A_p are the gross and aperture area of the collector, respectively. The gross collector area A_c is defined as the total area occupied by a collector and the aperture collector area A_p is the transparent frontal area. The + superscript indicates that only positive values of the terms in the square brackets are to be used. Thus, to produce useful gain greater than zero the absorbed radiation must be greater than the thermal losses. The useful gain from the collector based on the gross collector area is:

$$Q_u = A_c \left[S_c - U_L \left(T_{pm} - T_\alpha\right)\right]^+ \tag{9}$$

where S_c is the absorbed solar radiation per unit area based on the gross collector area, defined as:

$$S_c = S \frac{A_p}{A_c} \tag{10}$$

Since the radiation absorption and heat loss at the absorber plate is considered based on the aperture area in this analysis, it is convenient to make the aperture collector area the reference collector area of the useful gain. Then Equation 9 becomes:

$$Q_u = A_p \left[S - U_L' \left(T_{pm} - T_\alpha\right)\right]^+ \tag{11}$$

where U_L' is the overall heat loss coefficient based on the aperture area given by:

$$U_L' = U_L \frac{A_c}{A_p} \tag{12}$$

4.4 Absorbed solar radiation

The prediction of collector performance requires information on the solar energy absorbed by the collector absorber plate. The incident radiation has three different spatial distributions: beam radiation, diffuse radiation and ground-reflected radiation. Using the isotropic diffuse concept on an hourly basis, the absorbed radiation *S* is given by [10, 22]:

$$S = I_b R_b (\tau\alpha)_b + I_d (\tau\alpha)_d \left(\frac{1+\cos\beta}{2}\right) + \rho_g (I_b + I_d)(\tau\alpha)_g \left(\frac{1-\cos\beta}{2}\right) \quad (13)$$

where (1 + cos β)/2 and (1 - cos β)/2 are the view factors from the collector to the sky and from the collector to the ground, respectively. The subscripts *b*, *d* and *g* represent beam, diffuse and ground. *I* is the intensity of radiation on a horizontal surface, *(τα)* the transmittance-absorptance product that represents the effective absorptance of the cover-plate system and *β* the collector slope. ρ_g is the diffuse reflectance of ground and the geometric factor R_b is the ratio of beam radiation on the tilted surface to that on a horizontal surface. R_b is given by:

$$R_b = \frac{\cos\theta}{\cos\theta_z} \quad (14)$$

4.4.1 Reflection of radiation

For smooth surfaces the Fresnel expressions calculate the reflection of unpolarized radiation on passing from medium 1 with a refractive index n_1 to medium 2 with a refractive index n_2 [10, 22]:

$$r_\perp = \frac{\sin^2(\theta_2 - \theta_1)}{\sin^2(\theta_2 + \theta_1)} \quad (15)$$

$$r_\parallel = \frac{\tan^2(\theta_2 - \theta_1)}{\tan^2(\theta_2 + \theta_1)} \quad (16)$$

$$r = \frac{1}{2}(r_\perp + r_\parallel) \quad (17)$$

where ϑ_1 and ϑ_2 are the angles of incidence and refraction, as shown in Figure 13. Equation 15 represents the perpendicular component of unpolarized radiation $r_\perp$ and Equation 16 represents the parallel component of unpolarized radiation $r_\parallel$.

Parallel and perpendicular refer to the plane defined by the incident beam and the surface normal. Equation 17 then gives the reflection of unpolarized radiation as the average of the two components. The angles ϑ_1 and ϑ_2 are related to the indices of refraction by Snell's law:

$$\frac{n_1}{n_2} = \frac{\sin\theta_2}{\sin\theta_1} \tag{18}$$

Thus if the angle of incidence and refractive indices are known, Equations 15 through 18 are sufficient to calculate the radiation of the single interface.

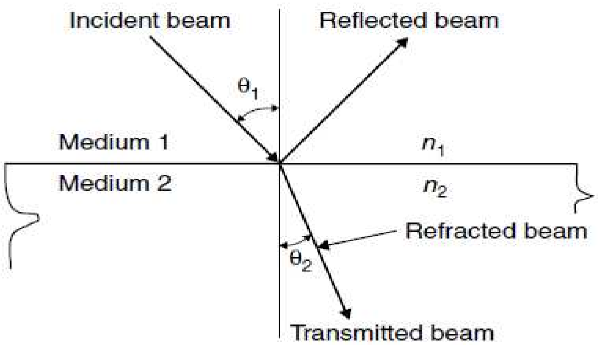

Figure 13: Angles of incidence and refraction [10]

4.4.2 Absorption by glazing

The absorption of radiation in a partially transparent medium is described by Bouguer's law, which is based on the assumption that the absorbed radiation is proportional to the local intensity in the medium and the distance the radiation has traveled in the medium. The transmittance of the medium is then [10, 22]:

$$\tau_\alpha = \exp\left(-\frac{KL}{\cos\theta_2}\right) \tag{19}$$

where K is the extinction coefficient which is assumed to be a constant in the solar spectrum and L is the thickness of the medium. The subscript α is a reminder that only absorption losses have been considered.

4.4.3 Optical properties of cover systems

The transmittance, reflectance and absorptance of a single cover, allowing for both reflection and absorption losses, can be determined by ray-tracing techniques. For the perpendicular and parallel components of polarization, the transmittance τ, reflectance ρ and absorptance α of the cover are [10, 22]:

$$\tau_{\perp} = \tau_{\alpha} \frac{1 - r_{\perp}}{1 + r_{\perp}} \frac{1 - r_{\perp}^{2}}{1 - \left(r_{\perp} \tau_{\alpha}\right)^{2}} \tag{20}$$

$$\rho_{\perp} = r_{\perp} \left[1 + \frac{\left(1 - r_{\perp}\right)^{2} \tau_{\alpha}^{2}}{1 - \left(r_{\perp} \tau_{\alpha}\right)^{2}} \right] \tag{21}$$

$$\alpha_{\perp} = \frac{\left(1 - \tau_{\alpha}\right)\left(1 - r_{\perp}\right)}{1 - r_{\perp} \tau_{\alpha}} \tag{22}$$

$$\tau_{\parallel} = \tau_{\alpha} \frac{1 - r_{\parallel}}{1 + r_{\parallel}} \frac{1 - r_{\parallel}^{2}}{1 - \left(r_{\parallel} \tau_{\alpha}\right)^{2}} \tag{23}$$

$$\rho_{\parallel} = r_{\parallel} \left[1 + \frac{\left(1 - r_{\parallel}\right)^{2} \tau_{\alpha}^{2}}{1 - \left(r_{\parallel} \tau_{\alpha}\right)^{2}} \right] \tag{24}$$

$$\alpha_{\parallel} = \frac{\left(1 - \tau_{\alpha}\right)\left(1 - r_{\parallel}\right)}{1 - r_{\parallel} \tau_{\alpha}} \tag{25}$$

For incident unpolarized radiation, the optical properties are found by the average of the two components:

$$\tau = \frac{1}{2}\left(\tau_{\perp} + \tau_{\parallel}\right) \tag{26}$$

$$\rho = \frac{1}{2}\left(\rho_{\perp} + \rho_{\parallel}\right) \tag{27}$$

$$\alpha = \frac{1}{2}\left(\alpha_{\perp} + \alpha_{\parallel}\right) \tag{28}$$

For a two-cover system, ray-tracing yields the following equations for transmittance and reflectance:

$$\tau = \frac{1}{2}\left(\tau_{\perp} + \tau_{\parallel}\right) = \frac{1}{2}\left[\left(\frac{\tau_2 \tau_1}{1 - \rho_2 \rho_1}\right)_{\perp} + \left(\frac{\tau_2 \tau_1}{1 - \rho_2 \rho_1}\right)_{\parallel}\right] \tag{29}$$

$$\rho = \frac{1}{2}\left[\left(\rho_2 + \frac{\tau\rho_1\tau_2}{\tau_1}\right)_{\perp} + \left(\rho_2 + \frac{\tau\rho_1\tau_2}{\tau_1}\right)_{\parallel}\right] \tag{30}$$

where subscripts *1* and *2* refer to inner and outer cover, respectively. It should be noted that the reflectance of the cover system depends upon which cover first intercepts solar radiation.

4.4.4 Equivalent angles of incidence for diffuse and ground-reflected radiation

The preceding analysis applies only to the beam component of solar radiation. Radiation incident on a collector also consists of scattered solar radiation from the sky and reflected solar radiation from the ground. The calculation can be simplified by defining an equivalent angle for beam radiation that gives the same transmittance as for diffuse and ground-reflected radiation.

If the diffuse radiation from the sky and the radiation reflected from the ground are both isotropic, then the transmittance of the glazing systems can be found by integrating the beam transmittance over the appropriate incidence angles. The effective incidence angle for diffuse radiation is [10, 22]:

$$\theta_{d,e} = 59.7 - 0.1388\beta + 0.001497\beta^2 \tag{31}$$

while the effective incidence angle for ground-reflected radiation is:

$$\theta_{g,e} = 90 - 0.5788\beta + 0.002693\beta^2 \tag{32}$$

where β is the solar collector slope.

4.4.5 Transmittance-absorptance product

Some of the radiation passing through the cover system is reflected back to the cover system while the remainder is absorbed at the plate. In turn, the reflected radiation from the plate will be partially reflected at the cover system and back to the plate. It is assumed that the reflection from the absorber plate is diffuse and unpolarized. The multiple reflection of diffuse radiation continues so that the fraction of the incident energy ultimately absorbed becomes [10, 22]:

$$(\tau\alpha) = \frac{\tau\alpha}{1-(1-\alpha)\rho_d} \tag{33}$$

where τ is the transmittance of the cover system at the desired angle, α is the angular absorptance of the absorber plate and ρ_d refers to the reflectance of the cover system for diffuse radiation incident from the bottom side.

Selective surfaces may exhibit similar behaviour concerning the angular dependence of solar absorptance. A polynomial expression for the angular dependence of transmittance-absorptance product for angles of incidence between 0 and 80° is given by:

$$\frac{\alpha}{\alpha_n} = 1 - 1.5879*10^{-3}\theta + 2.7314*10^{-4}\theta^2 - 2.3026*10^{-5}\theta^3 + \\ + 9.0244*10^{-7}\theta^4 - 1.8*10^{-8}\theta^5 + 1.7734*10^{-10}\theta^6 - 6.9937*10^{-13}\theta^7 \quad (34)$$

where the subscript n refers to the normal incidence and ϑ is in °C.

4.5 Heat loss from collector

In solar collectors, the solar energy absorbed by the absorber plate is distributed to useful gain and to thermal losses through the top, bottom, and edges. In this section, the equations for each loss coefficient are derived for a general configuration of the collector. In this analysis, the semi-gray model is employed for radiation heat transfer.

4.5.1 Collector overall heat loss

Heat loss from a solar collector consists of top heat loss through cover system and back and edge heat loss through back and edge insulation of the collector. With the assumption that all the losses are based on a common mean plate temperature T_{pm}, the overall heat loss from the collector can be represented as [10, 22]:

$$Q_{loss} = U_L A_c \left(T_{pm} - T_\alpha\right) \quad (35)$$

where U_L is the collector overall loss coefficient. The overall heat loss is the sum of the top, back, and edge losses:

$$Q_{loss} = Q_t + Q_b + Q_e \quad (36)$$

where the subscripts t, b and e represent for top, back and edge, respectively.

4.5.2 Top heat loss through the cover system

To evaluate the heat loss through the cover system, all of the convection and radiation heat transfer mechanisms between parallel plates and between the plate and the sky must be considered.

The collector model may have up to two covers which are made of either glass or plastic. In case of plastic covers that are partially transparent to infrared radiation, the direct radiation exchange between the plate and sky through the cover system must be considered while it is neglected for the glass covers since glass is opaque to infrared radiation. The net radiation method is applied to obtain the expression for the heat loss for the general cover system of flat plate solar collectors.

As shown in Figure 14, the net radiation method for a flat plate solar collector with two covers is used to derive the expression for the top heat loss from the collector plate to the ambient. The outgoing radiation flux from the covers can be written in terms of incoming fluxes as [10, 22, 23]:

$$q_{1,o} = \tau_{c1} q_{2,i} + \rho_{c1} q_{1,i} + \varepsilon_{c1} \sigma T_{c1}^{\ 4} \tag{37}$$

$$q_{2,o} = \tau_{c1} q_{1,i} + \rho_{c1} q_{2,i} + \varepsilon_{c1} \sigma T_{c1}^{\ 4} \tag{38}$$

$$q_{3,o} = \tau_{c2} q_{4,i} + \rho_{c2} q_{3,i} + \varepsilon_{c2} \sigma T_{c2}^{\ 4} \tag{39}$$

$$q_{4,o} = \tau_{c2} q_{3,i} + \rho_{c2} q_{4,i} + \varepsilon_{c2} \sigma T_{c2}^{\ 4} \tag{40}$$

where subscripts *c1* and *c2* represent cover 1 (inner cover) and cover 2 (outer cover) while τ, ρ and ε are the transmittance, reflectance and emittance of the covers and σ is the Stefan-Boltzmann constant. The incoming fluxes are related to outgoing fluxes by:

$$q_{1,i} = \rho_p q_{1,o} + \varepsilon_p \sigma T_{pm}^{\ 4} \tag{41}$$

$$q_{2,i} = q_{3,o} \tag{42}$$

$$q_{3,i} = q_{2,o} \tag{43}$$

$$q_{4,i} = \sigma T_s^{\ 4} \tag{44}$$

Applying the energy balance to two covers yields:

$$q_{1,i} - q_{1,o} + h_{c,pc1}\left(T_{pm} - T_{c1}\right) = q_{2,o} - q_{2,i} + h_{c,c1c2}\left(T_{c1} - T_{c2}\right) \quad (45)$$

$$q_{3,i} - q_{3,o} + h_{c,c1c2}\left(T_{c1} - T_{c2}\right) = q_{4,o} - q_{4,i} + h_{w}\left(T_{c2} - T_{\alpha}\right) \quad (46)$$

where $h_{c,pc1}$ and $h_{c,c1c2}$ are natural convection heat transfer coefficients between the plate and cover 1 and between cover 1 and cover 2, respectively. By solving the system of Equations 37 to 46, all the radiation fluxes and cover temperatures can be obtained for the given values of plate and sky temperatures. The top loss from the plate to the ambient can be calculated from:

$$Q_t = A_p\left[q_{c1,1,i} - q_{c1,1,o} + h_{c,pc1}\left(T_{pm} - T_{c1}\right)\right] \quad (47)$$

An empirical equation for top loss coefficient from the collector to the ambient, U_t, that can be used for both hand and computer calculations is [22]:

$$U_t = \left[\frac{N}{\dfrac{C}{T_{pm}}\left(\dfrac{T_{pm} - T_{\alpha}}{N+f}\right)^{e}} + \frac{1}{h_w}\right]^{-1} + \frac{\sigma\left(T_{pm} + T_{\alpha}\right)\left(T_{pm}^{\,2} + T_{\alpha}^{\,2}\right)}{\left(\varepsilon_p + 0.0059Nh_w\right)^{-1} + \dfrac{2N + f - 1 + 0.133\varepsilon_p}{\varepsilon_g} - N} \quad (48)$$

where σ is the Stefan-Boltzmann constant, N is the number of glass covers, β is the collector tilt in °C, ε_g is the emittance of glass, ε_p is the emittance of plate, T_α is the ambient temperature, T_{pm} is the mean plate temperature and h_w is the wind heat transfer coefficient. f, C and e are given by the following equations:

$$f = \left(1 + 0.089h_w - 0.1166h_w\varepsilon_p\right)\left(1 + 0.07866N\right) \quad (49)$$

$C = 520\left(1 - 0.000051\beta^2\right)$ for $0^\circ < \beta < 70^\circ$ (50)

(for $70^\circ < \beta < 90^\circ$ $\beta = 70^\circ$ is used)

$$e = 0.43\left(1 - 100/T_{pm}\right) \quad (51)$$

Both methods lead to nearly identical results.

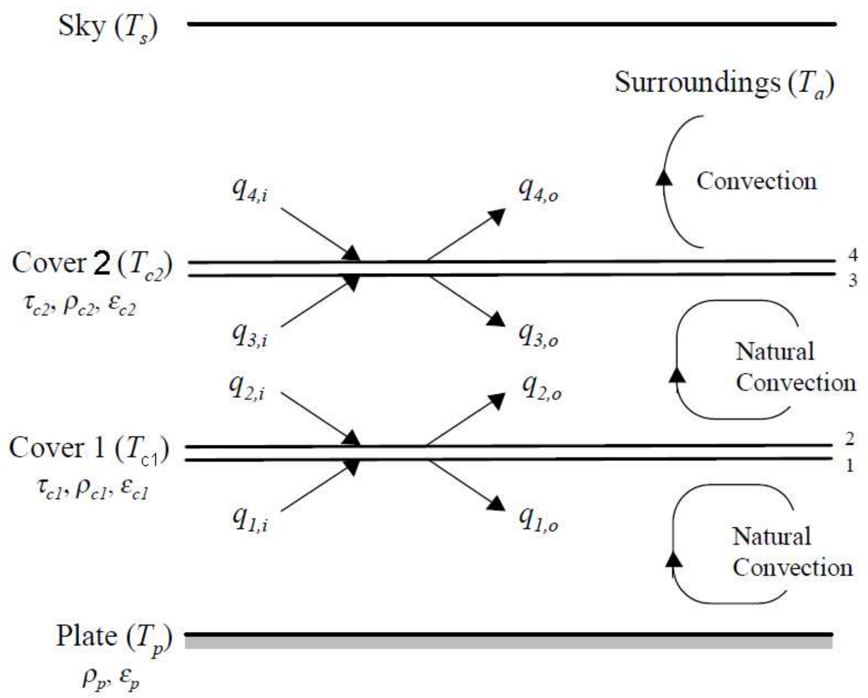

Figure 14: Net radiation method for two-cover collector [23]

4.5.3 Sky temperature

The radiation heat transfer from the plate to the sky is derived using the sky temperature T_s rather than the ambient temperature T_a. The sky can be considered as a blackbody at some equivalent sky temperature T_s to account for the facts that the atmosphere does not have a uniform temperature and that the atmosphere radiates only in certain wavelength band. T_s can be calculated using the equation as follows [10, 22, 24]:

$$T_s = T_\alpha \left[0.711 + 0.0056\mathrm{T}_{dp} + 0.000073\mathrm{T}_{dp}{}^2 + 0.013\cos(15t)\right]^{1/4} \tag{52}$$

where t is the hour from midnight. T_s and T_a are in K and T_{dp} is the dew point temperature in °C.

4.5.4 Wind convection coefficient

Wind convection coefficient h_w represents the convection heat loss from a flat plate exposed to outside winds. It is related to three dimensionless parameters, the Nusselt number *Nu*, the Reynolds number *Re* and the Prandtl number *Pr*, that are given by [10, 22, 23]:

$$Nu = \frac{h_w L_e}{k}, \qquad \mathrm{Re} = \frac{V L_e}{v}, \qquad \mathrm{Pr} = \frac{v}{\alpha} \tag{53}$$

where the characteristic length L_e is four times the plate area divided by the plate perimeter, V is the wind speed, k is the thermal conductivity, v is the kinematic viscosity and α is the thermal diffusivity of air. The wind convection coefficient can be calculated by [22]:

$$Nu = 0.86\,\mathrm{Re}^{1/2}\,\mathrm{Pr}^{1/3} \qquad (2\times10^4 < \mathrm{Re} < 10^6) \tag{54}$$

From this equation, an approximate equation, that is widely used, is derived for h_w:

$$h_w = 2.8 + 3V \tag{55}$$

4.5.5 Natural convection between parallel plates

For the prediction of the top loss coefficient, it is important to evaluate natural convection heat transfer between two parallel plates tilted at some angle to the horizon. The natural convection heat transfer coefficient h_c is related to three dimensionless parameters, the Nusselt number *Nu*, the Rayleigh number *Ra*, and the Prandtl number *Pr*, that are given by [10, 22]:

$$Nu = \frac{h_c L}{k}, \qquad Ra = \frac{g\beta_v \Delta T L^3}{v\alpha}, \qquad \mathrm{Pr} = \frac{v}{\alpha} \tag{56}$$

where L is the plate spacing, g is the gravitational constant, ΔT is the temperature difference between plates and β_v is the volumetric coefficient of expansion of air. The relationship between the Nusselt and the Rayleigh numbers for tilt angles from 0 to 75° is [23]:

$$Nu = 1 + 1.44\left[1 - \frac{1708[\sin(1.8\beta)]^{1.6}}{Ra\cos\beta}\right]\left[1 - \frac{1708}{Ra\cos\beta}\right]^{+} + \left[\left(\frac{Ra\cos\beta}{5830}\right)^{1/3} - 1\right]^{+} \tag{57}$$

4.5.6 Back and edge heat loss

The energy loss through the back of the collector is the result of the conduction through the back insulation and the convection and radiation heat transfer from the back of the collector to the ambient. Since the magnitudes of the thermal resistance of convection and radiation heat transfer are much smaller than that of conduction, it can be assumed that all thermal resistance from the back is due to the insulation. The back heat loss Q_b can be obtained from [10, 22]:

$$Q_b = \frac{k_b}{L_b} A_c \left(T_{pm} - T_\alpha\right) \quad (58)$$

where k_b and L_b are the back insulation thermal conductivity and thickness, respectively.

Assuming that there is one-dimensional sideways heat flow around the perimeter of the collector, the edge losses can be estimated by:

$$Q_e = \frac{k_e}{L_e} A_e \left(T_{pm} - T_\alpha\right) \quad (59)$$

where k_e and L_e are the edge insulation thermal conductivity and thickness, respectively while A_e is the edge area of the collector.

4.5.7 Overall heat loss coefficient

The overall loss coefficient U_L based on the gross collector area can be calculated from Equation 35 with the known values of the overall heat loss and the plate temperature. To derive an expression for the mean temperature of the absorber plate, it is necessary to know the overall heat loss coefficient based on the absorber area. Since the product of heat transfer coefficient and area is constant, it can be calculated from [10, 22]:

$$U_L' A_p = U_L A_c \quad (60)$$

where U_L' is the modified overall heat loss coefficient based on the aperture area of the collector.

4.6 Mean absorber plate temperature

To calculate the collector useful gain, it is necessary to know the mean temperature of the absorber plate that is a complicated function of temperature distribution on the absorber plate, bond conductivity, heat transfer inside of tubes and geometric configuration. To consider these factors along with the energy collected at the absorber plate and the heat loss, the collector efficiency factor and the collector heat removal factor are introduced.

4.6.1 Collector Efficiency Factor

The collector efficiency factor *F'* represents the temperature distribution along the absorber plate between tubes. Figure 15 illustrates the absorber plate-tube configuration of the collector model considered. With the assumption of negligible temperature gradient in the fin in the flow direction, the collector efficiency factor can be obtained by solving the classical fin problem. The distance between the tubes is *W*, the tube diameter is *D* and the sheet is thin with a thickness δ. The plate just above the tube is assumed to be at some local base temperature T_b. and the fin is *(W-D)/2* long. By applying energy balance on an elemental region of width *dx* and unit length in the flow direction the equation for the fin can be obtained as [10, 22]:

$$\frac{d^2T}{dx^2} = \frac{U_L'}{k\delta}\left(T - T_\alpha - \frac{S}{U_L'}\right) \tag{61}$$

where U_L' is the overall loss coefficient based on the aperture area. The two boundary conditions necessary to solve this second-order differential equation are symmetry at the centerline and the known base temperature:

$$\left.\frac{dT}{dx}\right|_{x=0} = 0, \qquad \left.T\right|_{x=(W-D)/2} = T_b \tag{62}$$

The energy conducted to the region of the tube per unit of length in the flow direction can be found by applying Fourier's law at the fin base:

$$q_{fin}' = (W - D)F\left[S - U_L'(T_b - T_\alpha)\right] \tag{63}$$

where *F* is the standard fin efficiency for straight fins with rectangular profile and defined as:

$$F = \frac{\tanh\left[m(W-D)/2\right]}{m(W-D)/2} \tag{64}$$

and *m* is a parameter of the fin-air arrangement defined as:

$$m = \sqrt{\frac{U_L'}{k\delta}} \tag{65}$$

The useful gain of the collector also includes the energy collected above the tube region. The energy gain for this region is:

$$q_{tube}' = D\left[S - U_L'(T_b - T_\alpha)\right] \tag{66}$$

and the useful gain for the tube and fin per unit of depth in the flow direction is the sum of q_{fin}' and q_{tube}':

$$q_u' = [(W-D)F + D][S - U_L'(T_b - T_\alpha)] \tag{67}$$

Ultimately, the useful gain must be transferred to the fluid. The resistance to heat flow to the fluid results from the bond and the tube-to-fluid resistance. The useful gain per unit of length in the flow direction can be expressed as:

$$q_u' = \frac{T_b - T_f}{\dfrac{1}{h_{fi}\pi D_i} + \dfrac{1}{C_b}} \tag{68}$$

where D_i is the inner diameter of a tube, h_{fi} is the forced-convection heat transfer coefficient inside of tubes, T_f is the local fluid temperature and C_b is the bond conductance. By eliminating T_b from Equations 67 and 68 and by introducing the collector efficiency factor *F'*, an expression for the useful gain is obtained:

$$q_u' = WF'\left[S - U_L'(T_f - T_\alpha)\right] \tag{69}$$

where the collector efficiency factor *F'* is defined as:

$$F' = \frac{1/U_L'}{W\left[\dfrac{1}{U_L'[D + (W-D)F]} + \dfrac{1}{C_b} + \dfrac{1}{\pi D_i h_{fi}}\right]} \tag{70}$$

A physical interpretation for *F'* results from examining Equation 70. At a particular location, the collector efficiency factor represents the ratio of the actual useful energy gain to the useful gain that would result if the collector absorbing surface had been at the local fluid temperature.

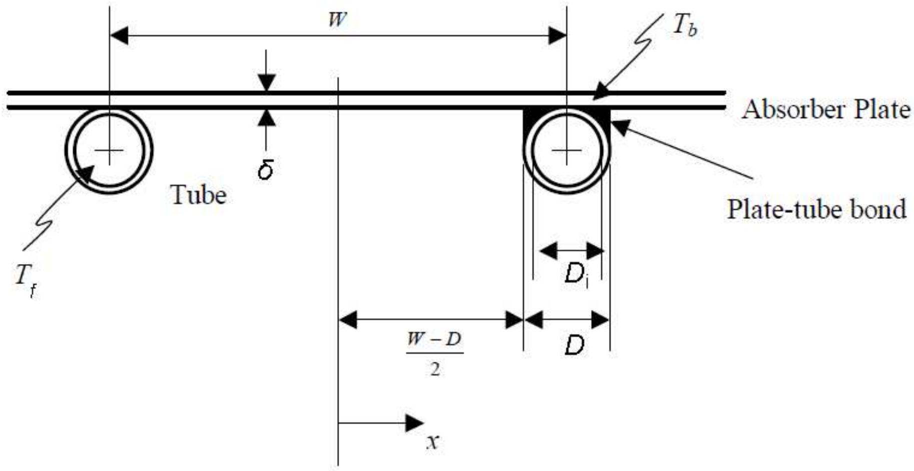

Figure 15: Geometric configuration of the absorber plate-tube [23]

4.6.2 Temperature distribution in flow direction

The useful gain per unit flow length is ultimately transferred to the fluid. The fluid enters the collector at temperature T_{fi} and increases in temperature until at the exit it is T_{fo}. An expression of the energy balance on the fluid flowing through a single tube of length dy is [10, 22]:

$$\dot{m} C_p \frac{dT_f}{dy} - nWF' \left[S - U_L' \left(T_f - T_\alpha \right) \right] = 0 \tag{71}$$

where $\dot{m}$ is the total collector flow rate, C_p is the specific heat capacity of the fluid at constant pressure, n is the number of parallel tubes and T_f is the temperature of the fluid at any location y. If we assume that F' and U_L are independent of position, then the solution for T_f is:

$$\frac{T_f - T_\alpha - S/U_L}{T_{fi} - T_\alpha - S/U_L} = \exp\left(-\frac{U_L' nWF' y}{\dot{m} C_p} \right) \tag{72}$$

If the collector length is L in the flow direction, then the outlet fluid temperature T_{fo} is found by substituting L for y in Equation 72. The quantity nWL is the collector area:

$$\frac{T_{fo} - T_\alpha - S/U_L'}{T_{fi} - T_\alpha - S/U_L'} = \exp\left(-\frac{A_p U_L' F}{\dot{m} C_p} \right) \tag{73}$$

4.6.3 Collector heat removal factor and flow factor

The collector heat removal factor F_R is a quantity that relates the actual useful energy gain of a collector to the maximum possible useful gain if the whole collector surface were at the fluid inlet temperature. In equation form it is [10, 22]:

$$F_R = \frac{\overset{*}{m} C_p \left(T_{fo} - T_{fi}\right)}{A_p\left[S - U_L'\left(T_{fi} - T_\alpha\right)\right]} \tag{74}$$

By using Equation 73 to substitute T_{fo}, the collector heat removal factor can be expressed as:

$$F_R = \frac{\dot{m} C_p}{A_p U_L'}\left[1 - \exp\left(-\frac{A_p U_L' F'}{\dot{m} C_p}\right)\right] \tag{75}$$

It is also convenient to define the collector flow factor F'' as the ratio of the collector heat removal factor to the collector efficiency factor. Thus:

$$F'' = \frac{F_R}{F'} = \frac{\dot{m} C_p}{A_c U_L F'}\left[1 - \exp\left(-\frac{A_c U_L F'}{\dot{m} C_p}\right)\right] \tag{76}$$

This collector flow factor is a function of a single variable, the dimensionless collector capacitance rate $\dot{m} C_p / A_c U_L F'$.

The quantity F_R is equivalent to the effectiveness of a conventional heat exchanger, which is defined as the ratio of the actual heat transfer to the maximum possible heat transfer. The maximum possible useful energy gain in a solar collector occurs when the whole collector is at the inlet fluid temperature; heat losses to the surroundings are then at a minimum. The collector heat removal factor times this maximum possible useful energy gain is equal to the actual useful energy gain Q_u:

$$Q_U = A_p F_R\left[S - U_L'\left(T_{fi} - T_\alpha\right)\right]^+ \tag{77}$$

With it, the useful energy gain is calculated as a function of the inlet fluid temperature. This is a convenient representation when analyzing solar energy systems since the inlet fluid temperature is usually known.

4.6.4 Mean fluid and plate temperatures

To evaluate collector performance, it is necessary to know the overall loss coefficient and the internal fluid heat transfer coefficients. However, both U_L and h_{fi} are to some degree functions of temperature. The mean fluid temperature can be found by [10, 22]:

$$T_{fm} = T_{fi} + \frac{Q_U / A_p}{F_R U_L'}\left(1 - F''\right) \tag{78}$$

This is the proper temperature for evaluating fluid properties. The mean plate temperature will always be greater than the mean fluid temperature due to the heat transfer resistance between the absorbing surface and the fluid. If we equate Equations 11 and 77 and solve for the mean plate temperature, it is defined as:

$$T_{pm} = T_{fi} + \frac{Q_U / A_p}{F_R U_L'}\left(1 - F_R\right) \tag{79}$$

Equation 79 can be solved in an iterative manner with Equation 48. First an estimate of the mean plate temperature is made from which U_L is calculated. With approximate values of F_R, F'' and Q_u, a new mean plate temperature is obtained from Equation 79 and used to find a new value for the loss coefficient. The new value of U_L is used to refine F_R and F'' and the process is repeated until the mean plate temperature is found.

4.6.5 Forced convection inside of tubes

For fully developed turbulent flow inside of tubes (Re>2300), the Nusselt number can be obtained from Gnielinsky correlation [10, 22, 23]:

$$Nu_{long} = \frac{(f/8)(\mathrm{Re}_{tube} - 1000)\mathrm{Pr}}{1 + 12.7\sqrt{f/8}\left(\mathrm{Pr}^{2/3} - 1\right)} \tag{80}$$

where Darcy friction factor f for smooth surface is calculated from Petukhov relation given by:

$$f = \left(0.79 \ln \mathrm{Re} - 1.64\right)^{-2} \tag{81}$$

For short tubes with a sharp-edged entry, the McAdams relation can be used:

$$Nu = Nu_{long}\left[1+\left(\frac{D}{L}\right)^{0.7}\right] \tag{82}$$

where *D* and *L* is inner diameter and length of a tube.

For laminar flow inside of tubes, the local Nusselt number for the case of short tubes and constant heat flux is given by:

$$Nu = Nu_{long} + \frac{a(\mathrm{Re}\,\mathrm{Pr}\,D/L)^m}{1+b(\mathrm{Re}\,\mathrm{Pr}\,D/L)^n} \tag{83}$$

With the assumption that the flow inside of tubes is fully developed, the values of Nu_{long}, *a*, *b*, *m*, and *n* are 4.4, 0.00172, 0.00281, 1.66 and 1.29, respectively, for the constant heat flux boundary condition. The friction factor *f* for fully developed laminar flow inside of a circular tube can be calculated from:

$$f = \frac{64}{\mathrm{Re}} \tag{84}$$

4.7 Thermal performance of collectors

The thermal performance of a flat plate collector can be represented by the instantaneous efficiency. The instantaneous collector efficiency *n* is a measure of collector performance and is defined as the ratio of the useful gain over some specified time period to the incident solar energy over the same time period [10, 22]:

$$\eta = \frac{\int Q_u\,dt}{A_c \int I_T\,dt} \tag{85}$$

where I_T is the intensity of incident solar radiation. By introducing the Equation 77 based on the gross collector area, the instantaneous efficiency becomes:

$$\eta = \frac{Q_u}{A_c I_T} = \left[F_R(\tau\alpha) - F_R U_L \frac{(T_{fi}-T_a)}{I_T}\right]^+ \tag{86}$$

where the absorbed energy S_c based on the gross collector area has been replaced by:

$$S_c = I_T(\tau\alpha) \tag{87}$$

($\tau\alpha$) is the effective transmittance-absorptance product based on the gross collector area defined as:

$$\left(\tau\alpha\right) = \frac{SA_p}{I_T A_c} = \left(\tau\alpha\right)_{avg} \frac{A_p}{A_c} \tag{88}$$

where $(\tau\alpha)_{avg}$ is the transmittance-absorptance product averaged for beam, diffuse and ground-reflected radiation. SA_p is the solar energy absorbed at absorber surface and $I_T A_c$ is the total solar energy incident on the gross area of the collector. In Equation 81, two important parameters, $F_R(\tau\alpha)$ and $F_R U_L$, describe the collector performance. $F_R(\tau\alpha)$ indicates how energy is absorbed by the collector while $F_R U_L$ is an indication of how energy is lost from the collector.

4.8 Algorithm of the simulation model

Programming language MATLAB was used to develop the algorithm of the simulation model for flat plate solar collectors.

First, the algorithm calculates the optical losses of the incident solar radiation on the absorber plate and consequently the absorbed radiation by the plate (Equation 13). The next step is the use of Equations 36, 48, 58 and 59 to find the top heat loss through the cover system, the back and edge heat loss through back and edge insulation and the overall heat loss of the collector. The calculation of heat loss is made with an estimated value of the mean plate temperature. By calculating optical and thermal losses, the useful energy gain of the collector (Equation 8), the collector heat removal and flow factors (Equations 75, 76) are also found. Simultaneously, a new value of mean plate temperature is obtained from Equation 79 and compared to the estimated one. The process is repeated until desired accuracy is reached. Finally, the instantaneous efficiency of the collector is found using Equation 86. The flowchart of the algorithm is shown in Figure 16.

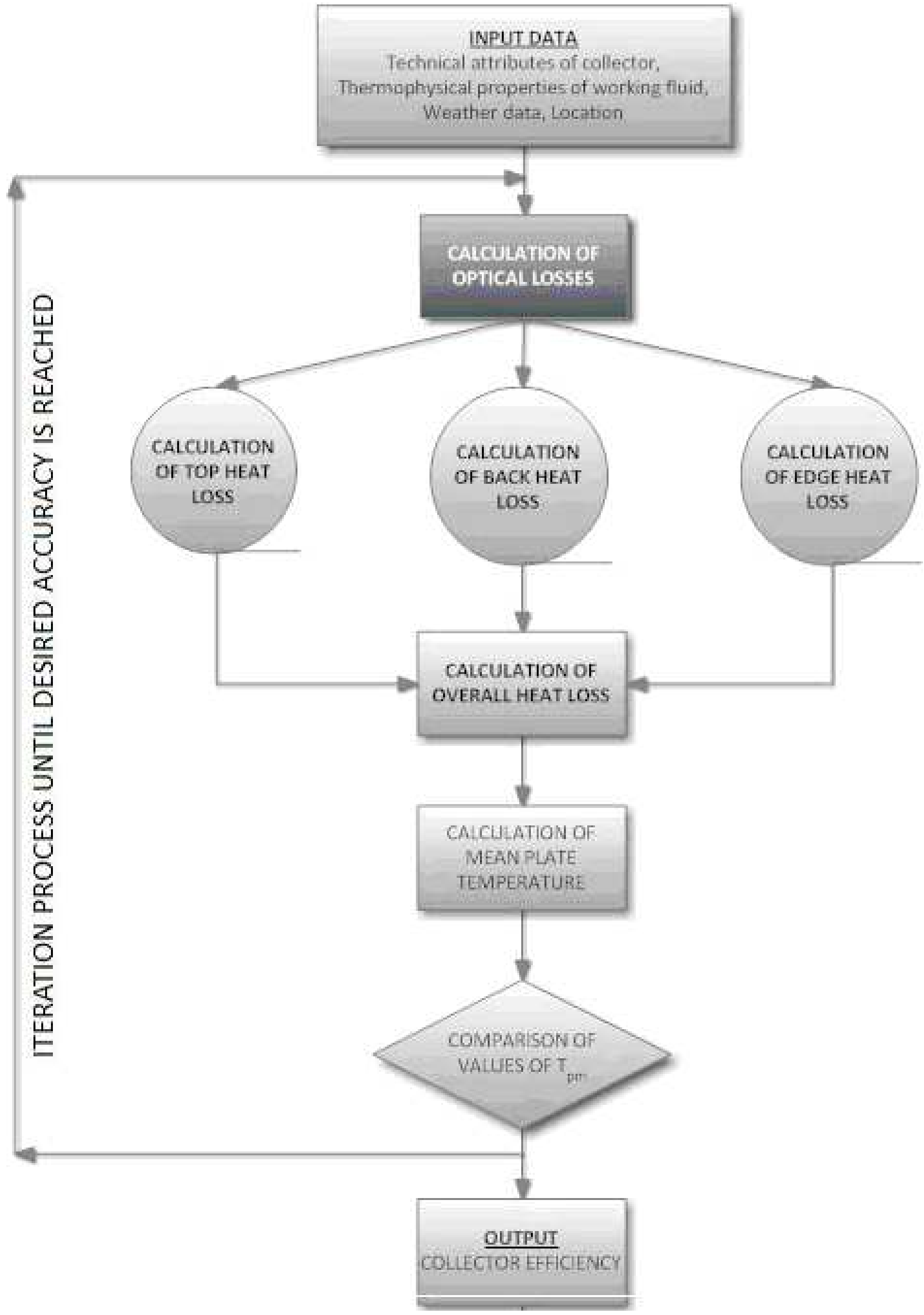

Figure 16: Flowchart of algorithm

5 Results

In this chapter, the simulation of a flat plate collector is performed. Given the technical attributes of the specific flat plate collector under test, data about the location where it will be installed and the weather data of the location, the simulation program provides the collector efficiency as a function of the ratio of the temperature difference between the fluid and the ambient to the incident solar radiation.

Test conditions and collector configurations are summarized in Table 4. The collector under test is a flat plate solar collector which uses water as the working fluid and its cover is made of glass. The performance of the collector was simulated using local and climatic conditions of Thessaloniki, Greece during summer period.

The simulation program is run in MATLAB. A plot of the instantaneous efficiency of the collector with the above technical attributes at the defined weather and local conditions is shown in Figure 17 as a function of $(T_{in}-T_{\alpha})/I_T$.

The maximum efficiency of the collector is 65.87% while the slope of the efficiency curve is 5.19. Thus, the equation describing the collector efficiency curve is:

$$\eta = 0.6587 - 5.32\frac{T_{in} - T_a}{I_T}$$

As shown from the above analysis, the MATLAB-based simulation program is very useful since it can predict the average performance of the collector very well and consequently minimize time for new, optimum collector design.

Location and weather conditions	Day of the year (starting from January 1st)	*190*
	Standard meridian for local time zone	*330 °*
	Longitude of location	*337.1 °*
	Local standard time (in hours)	*12*
	Latitude of location	*40.65 °*
Test conditions	Intensity of beam radiation	*1000 W/m^2*
	Intensity of diffuse radiation	*0 W/m^2*
	Slope of collector	*45 °*
	Ambient temperature	*20 °C*
	Wind speed	*2 m/s*
	Ground reflectance	*0.4*
Collector dimensions	Collector length	*2.491 m*
	Collector width	*1.221 m*
	Collector thickness	*0.079 m*
	Absorber plate length	*2.4 m*
	Absorber plate width	*1.137 m*
Cover	Number of covers	*1*
	Material	*Glass*
	Index of refraction	*1.526*
Plate	Emittance	*0.88*
	Extinction coefficient of cover	*5 m^{-1}*
	Thickness of cover	*0.005 m*
	Emittance	*0.1*
	Thermal conductivity	*380 W/(m*K)*
	Thickness	*0.0002 m*
	Absorptance at normal incidence	*0.953*
Back & edge insulation	Back insulation thermal conductivity	*0.03 W/(m*K)*
	Back insulation thickness	*0.03 m*
	Edge insulation thermal conductivity	*0.03 W/(m*K)*
	Edge insulation thickness	*0.03 m*
Tubes & fluid	Tube diameter	*0.02 m*
	Inner diameter of tube	*0.016 m*
	Bond conductance	*400 W/(m*K)*
	Working fluid	*Water*
	Total collector flow rate	*0.07877 kg/s*
	Distance between tubes	*0.1 m*
	Length of tube	*2 m*

Table 4: Test conditions and specification of flat plate solar collector under test

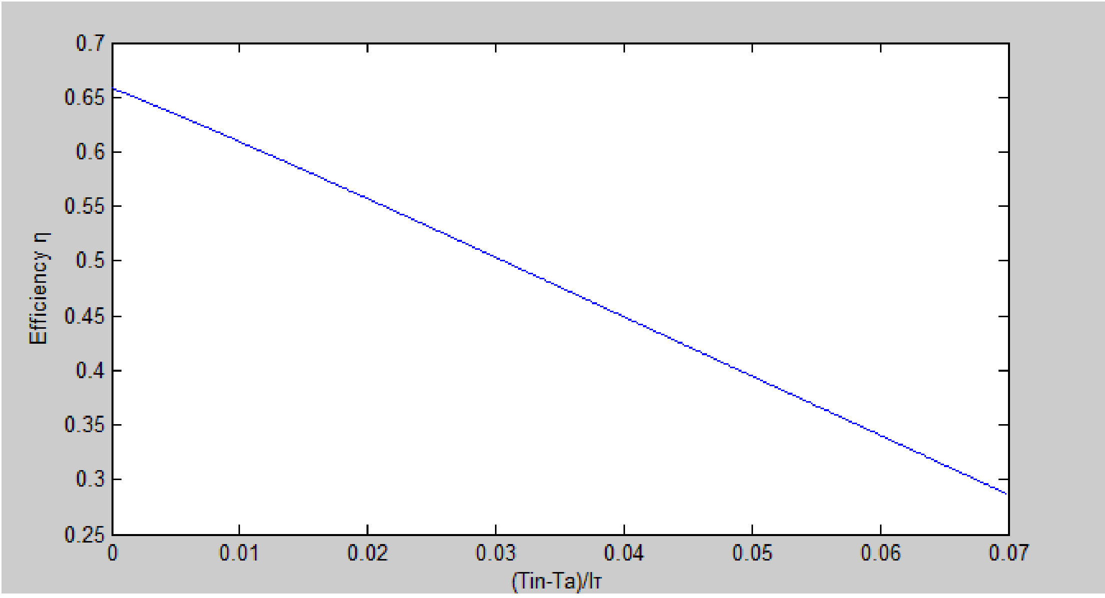

Figure 17: Calculated efficiency of collector under test

6 Conclusions

An analytical study has been conducted to develop a simulation model for flat plate solar collectors. The model is based on established theory about solar radiation absorption and optical losses, heat loss, thermodynamics and surface temperature distribution.

The predicted collector performance by the simulation model is very close to the real collector performance, given a specific collector. The slight differences between the predicted and the actual performance may come from the deviation between the actual environmental conditions and the assumed ones in the model process or from lack of information about the optical properties of the absorber plate. Even if the meteorological data used in the simulation are very accurate, the constant weather changes cannot be taken into account. However, the average instantaneous efficiency of the collector can be calculated with great accuracy.

Nomenclature

A_c	Gross collector area
A_e	Edge area of collector
A_p	Aperture area of collector
C_b	Tube-plate bond conductance
C_p	Specific heat capacity of the fluid at constant pressure
D	Tube diameter
D_i	Inner tube diameter
E	Equation of time
F	Standard fin efficiency
F’	Collector efficiency factor
F’’	Collector flow factor
F_R	Collector heat removal factor
f	Darcy friction factor
g	Gravitational constant
h_c	Natural convection heat transfer coefficient
h_{fi}	Forced-convection heat transfer coefficient inside of tubes
h_w	Wind heat transfer coefficient
I_b	Intensity of beam radiation
I_d	Intensity of diffuse radiation
I_T	Intensity of incident solar radiation
K	Extinction coefficient
k	Thermal conductivity
k_b	Back insulation thermal conductivity
k_e	Edge insulation thermal conductivity
L	Characteristic length
L_b	Back insulation thickness

L_e Edge insulation thickness

L_{loc} Longitude of the location in question

L_{st} Standard meridian for the local time zone

m Parameter of the fin-air arrangement

$\dot{m}$ Total collector flow rate

N Number of covers

Nu Nusselt number

n Day of the year

n_1 Refractive index of medium 1

n_2 Refractive index of medium 2

r Reflection of radiation

Pr Prandtl number

Q_b Back heat loss from the collector

Q_e Edge heat loss from the collector

Q_{loss} Overall heat loss from the collector

Q_t Top heat loss from the collector

Q_u Useful energy gain of the collector

q Radiation flux

R_b Geometric factor

Ra Rayleigh number

Re Reynolds number

S Solar radiation absorbed by the collector per unit area of absorber

S_c Solar radiation absorbed by the collector per unit area based on the gross collector area

T_α Ambient temperature

T_b Fin base temperature

T_c Temperature of the cover

T_{dp} Dew point temperature

T_{fm} Mean fluid temperature

T_{pm} Mean absorber plate temperature

T_s Sky temperature

t Hour from midnight

U_L Overall loss coefficient of the collector based on gross collector area

U_L' Overall loss coefficient of the collector based on aperture area

U_t Top loss coefficient from the collector

V Wind speed

v Kinematic viscosity

W Distance between the tubes

α Absorptance

α_n Absorptance at normal incidence

α_s Solar altitude angle

β Slope of the collector

β_v Volumetric coefficient of expansion of air

γ Surface azimuth angle

γ_s Solar azimuth angle

δ Declination

ε Emittance

ε_g Emittance of glass

ε_p Emittance of the plate

η Instantaneous efficiency of the collector

θ Angle of incidence

θ_2 Angle of refraction

$\theta_{d,e}$ Effective incidence angle for diffuse radiation

$\theta_{g,e}$ Effective incidence angle for ground-reflected radiation

θ_z Zenith angle

ρ Reflectance

ρ_d	Reflectance for diffuse radiation
ρ_g	Reflectance of ground
σ	Stefan-Boltzmann constant
τ	Transmittance
τ_α	Transmittance due to absorption of radiation
$(\tau\alpha)$	Transmittance-absorptance product
ϕ	Latitude of the location in question
ω	Hour angle

Appendix

The flat plate collector simulation program is a program that can help solar engineers design and test flat plate solar collectors. It has been developed so that most details of the collector configuration can be specified. The program has been developed using MATLAB. The test conditions and collector configurations are inserted into the program by a Microsoft Office Excel file (Inputs.xls). The program is then run in MATLAB using the command *solarcollector* and provides the graphical presentation of the instantaneous collector efficiency as a function of $(T_{in}-T_{\alpha})/I_T$. The MATLAB code of the program is the following.

MATLAB code

```
inputs=xlsread('Inputs.xls','B:B'); %inputs from Excel file
n=inputs(1);    %day of the year
Lst=inputs(2); %standard meridian for local time zone
Lloc=inputs(3); %longitude of location
standardtime=inputs(4); %local standard time
f=inputs(5)*pi/180; %latitude of location
b=inputs(6)*pi/180; %slope of collector
n1=inputs(7);   %index of refraction of medium 1
n2=inputs(8);   %index of refraction of medium 2
K=inputs(9);    %extinction coefficient of cover
L=inputs(10);   %thickness of cover
Ib=inputs(11);  %intensity of beam radiation
Id=inputs(12);  %intensity of diffuse radiation
V=inputs(13);   %wind speed
N=inputs(14);   %number of covers
ep=inputs(15);  %emittance of plate
eg=inputs(16);  %emittance of glass
```

```
T=inputs(17)+273.15;    %ambient temperature
lcoll=inputs(18);   %collector length
wcoll=inputs(19);   %collector width
tcoll=inputs(20);   %collector thickness
labs=inputs(21);    %absorber plate length
wabs=inputs(22);    %absorber plate width
kb=inputs(23);  %back insulation thermal conductivity
Lb=inputs(24);  %back insulation thickness
ke=inputs(25);  %edge insulation thermal conductivity
Le=inputs(26);  %edge insulation thickness
kapa=inputs(27);    %plate thermal conductivity
delta=inputs(28);   %plate thickness
W=inputs(29);   %distance between tubes
D=inputs(30);   %tube diameter
Di=inputs(31);  %inner diameter of tube
Cb=inputs(32);  %bond conductance
ltube=inputs(33);   %length of tube
alfa=inputs(34);    %thermal diffusivity of air
m=inputs(35);   %total collector flow rate
an=inputs(36);  %absorptance of plate at normal incidence
pg=inputs(37);  %ground reflectance
Ac=lcoll*wcoll; %gross collector area
Ap=labs*wabs;   %aperture collector area
Ae=(lcoll+wcoll)*tcoll; %edge collector area
d=23.45*pi/180*sin(360*(284+n)*pi/(365*180));   %declination angle
g=0;    %surface azimuth angle
B=(n-1)*pi*360/(365*180);   %angle B
E=229.2*(0.000075+0.001868*cos(B)-0.032077*sin(B)-0.014615*cos(2*B)-
```

```
        0.04089*sin(2*B));  %equation of time
solartime=standardtime+(4*(Lst-Lloc)+E)/60; %solar time
w=15*(solartime-12)*pi/180;   %hour angle
as=asin(cos(w)*cos(d)*cos(f)+sin(d)*sin(f));    %solar altitude angle
if (cos(w)>tan(d)/tan(f))
  gs=asin(cos(d)*sin(w)/cos(as));    %solar azimuth angle
else
  if (solartime<12)
    gs=-pi+abs(asin(cos(d)*sin(w)/cos(as)));
  else
    gs=pi-asin(cos(d)*sin(w)/cos(as));
  end
end
thz=acos(cos(f)*cos(d)*cos(w)+sin(f)*sin(d));   %solar zenith angle
th1=acos(sin(d)*sin(f)*cos(b)-sin(d)*cos(f)*sin(b)*cos(g)+
        cos(d)*cos(f)*cos(b)*cos(w)+cos(d)*sin(f)*sin(b)*cos(g)*cos(w)+
        cos(d)*sin(b)  *sin(g)*sin(w));  %angle of incidence
Rb=cos(th1)/cos(thz);  %geometric factor
th2=asin(n1/n2*sin(th1));   %angle of refraction
ta=exp(-K*L/cos(th2));  %transmittance, only absorption losses considered
rpe=(sin(th2-th1))^2/(sin(th2+th1))^2;  %reflection, perpendicular component of
        polarization
rpa=(tan(th2-th1))^2/(tan(th2+th1))^2;  %reflection, parallel component of
        polarization
tpe=ta*(1-rpe)/(1+rpe)*(1-rpe^2)/(1-(rpe*ta)^2);    %transmittance, perpendicular
        component of polarization
tpa=ta*(1-rpa)/(1+rpa)*(1-rpa^2)/(1-(rpa*ta)^2);    %transmittance, parallel
        component of polarization
```

```
t=(tpe+tpa)/2;  %transmittance
thd1=(59.7-0.1388*b*180/pi+0.001497*(b*180/pi)^2)*pi/180;   %effective incidence
        angle for diffuse radiation
thg1=(90-0.5788*b*180/pi+0.002693*(b*180/pi)^2)*pi/180; %effective incidence
        angle for ground-reflected radiation
thd2=asin(n1/n2*sin(thd1)); %effective angle of refraction for diffuse radiation
thg2=asin(n1/n2*sin(thg1)); %effective angle of refraction for ground-reflected
        radiation
tad=exp(-K*L/cos(thd2));    %transmittance, only absorption losses considered for
        diffuse radiation
tag=exp(-K*L/cos(thg2));    %transmittance, only absorption losses considered for
        ground-reflected radiation
rped=(sin(thd2-thd1))^2/(sin(thd2+thd1))^2; %reflection, perpendicular component
        of polarization for diffuse radiation
rpad=(tan(thd2-thd1))^2/(tan(thd2+thd1))^2; %reflection, parallel component of
        polarization for diffuse radiation
rpeg=(sin(thg2-thg1))^2/(sin(thg2+thg1))^2; %reflection, perpendicular component
        of polarization for ground-reflected radiation
rpag=(tan(thg2-thg1))^2/(tan(thg2+thg1))^2; %reflection, parallel component of
        polarization for ground-reflected radiation
tped=tad*(1-rped)/(1+rped)*(1-rped^2)/(1-(rped*tad)^2); %transmittance,
        perpendicular component of polarization for diffuse radiation
tpad=tad*(1-rpad)/(1+rpad)*(1-rpad^2)/(1-(rpad*tad)^2); %transmittance, parallel
        component of polarization for diffuse radiation
pped=rped*(1+((1-rped)^2*tad^2)/(1-(rped*tad)^2));  %reflectance, perpendicular
        component of polarization for diffuse radiation
ppad=rpad*(1+((1-rpad)^2*tad^2)/(1-(rpad*tad)^2));  %reflectance, parallel
        component of polarization for diffuse radiation
```

```
tpeg=tag*(1-rpeg)/(1+rpeg)*(1-rpeg^2)/(1-(rpeg*tag)^2); %transmittance,
    perpendicular component of polarization for ground-reflected radiation
tpag=tag*(1-rpag)/(1+rpag)*(1-rpag^2)/(1-(rpag*tag)^2); %transmittance, parallel
    component of polarization for ground-reflected radiation
td=(tped+tpad)/2;   %transmittance for diffuse radiation
pd=(pped+ppad)/2;   %reflectance for diffuse radiation
tg=(tpeg+tpag)/2;   %transmittance for ground-reflected radiation
a=(1+0.0020345*(th1*180/pi)-0.000199*(th1*180/pi)^2+0.000005324*
    (th1*180/pi)^3-0.00000004799*(th1*180/pi)^4)*an;    %absorptance
ad=(1+0.0020345*(thd1*180/pi)-0.000199*(thd1*180/pi)^2+0.000005324*
    (thd1*180/pi)^3-0.00000004799*(thd1*180/pi)^4)*an;   %absorptance for
    diffuse radiation
ag=(1+0.0020345*(thg1*180/pi)-0.000199*(thg1*180/pi)^2+0.000005324*
    (thg1*180/pi)^3-0.00000004799*(thg1*180/pi)^4)*an;      %absorptance  for
    ground-reflected radiation
tab=t*a/(1-(1-a)*pd);   %transmittance-absorptance product for beam radiation
tadd=td*ad/(1-(1-ad)*pd);   %transmittance-absorptance product for diffuse
    radiation
tagg=tg*ag/(1-(1-ag)*pd);   %transmittance-absorptance product for ground-
    reflected radiation
taavg=(tab+tadd+tagg)/3;    %average transmittance-absorptance product
S=Ib*Rb*tab+Id*tadd*(1+cos(b))/2+pg*(Ib+Id)*tagg*(1-cos(b))/2;  %solar radiation
    absorbed
hw=2.8+3*V;  %wind heat transfer coefficient
sb=5.6704*10^-8;    %Stefan-Boltzmann constant
ef=(1+0.089*hw-0.1166*hw*ep)*(1+0.07866*N);   %f
if (b*180/pi<70)
   C=520*(1-0.000051*(b*180/pi)^2);    %C
```

```
else
   C=520*(1-0.000051*70^2);
end
Tpm=zeros(700,1);    %mean plate temperature
Tfm=zeros(700,1);    %mean fluid temperature
eff=zeros(700,1);    %collector efficiency
x=zeros(700,1);  %temperature difference between inlet fluid and ambient to
          incident solar radiation
for i=1:700,
   Tpm1=Tin+10;    %initial guess of mean plate temperature
   Cp=-0.0000854235*Tpm1^3+0.09488036*Tpm1^2-34.2228*Tpm1+8212.82;
          %specific heat capacity of water
   visc=(0.0000001406*Tpm1^2-0.0001024062*Tpm1+0.01895682)/(-0.003284948*
          Tpm1^2+1.687644*Tpm1+785.6677);   %kinematic viscosity
   Re=2*m*Di/(1000*pi*Di^2*visc）;  %Reynolds number
   Pr=visc/alfa;   %Prandtl number
   if (Re>2300)
      friction=(0.79*log(Re)-1.64)^-2;    %Darcy friction factor
      Nulong=(friction/8)*(Re-1000)*Pr/(1+12.7*sqrt(friction/8)*(Pr^(2/3)-1));
      Nu=Nulong*(1+(Di/ltube)^0.7); %Nusselt number
   else
      Nu=4.4+0.00172*(Re*Pr*Di/ltube)^1.66/(1+0.00281*(Re*Pr*Di/ltube)^1.29);
   end
   thcond=-0.00000981358*Tpm1^2+0.007536807*Tpm1-0.7674181;    %thermal
          conductivity of water
   hfi=Nu*thcond/Di;  %forced-convection heat transfer coefficient inside of tubes
   e=0.43*(1-100/Tpm1);    %e
   Ut=(N/((C/Tpm1*((Tpm1-T)/(N+ef))^e)+1/hw))^-1+
```

```
    (sb*(Tpm1+T)*(Tpm1^2+T^2))/((ep+0.00591*N*hw)^-1+(2*N+ef-1+
    0.133*ep)/eg-N);   %top loss coefficient from the collector plate to the
    ambient
Qt=Ac*Ut*(Tpm1-T);  %top heat loss
Qb=kb/Lb*Ac*(Tpm1-T);   %back heat loss
Qe=ke/Le*Ae*(Tpm1-T);   %edge heat loss
QL=Qt+Qb+Qe;    %overall heat loss
UL=QL/(Ac*(Tpm1-T));    %overall heat loss coefficient
UL2=UL*Ac/Ap;   %modified overall heat loss coefficient
mi=(UL2/(kapa*delta))^0.5;  %parameter of the fin-air arrangement
F=tanh(mi*(W-D)/2)/(mi*(W-D)/2);    %standard fin efficiency
F1=(1/UL2)/(W*(1/(UL2*(D+(W-D)*F))+1/Cb+1/(pi*Di*hfi)));  %collector
    efficiencty factor F'
FR=m*Cp/(Ap*UL2)*(1-exp(-Ap*UL2*F1/(m*Cp)));   %collector heat removal
    factor
Qu=Ap*(S-UL2*(Tpm1-T));  %useful gain from the collector
Tpm2=Tin+Qu/(Ap*FR*UL2)*(1-FR); %mean plate temperature
while(abs(Tpm1-Tpm2)>0.1)
  Tpm1=Tpm2;
  Cp=-0.0000854235*Tpm1^3+0.09488036*Tpm1^2-34.2228*Tpm1+8212.82;
  visc=(0.0000001406*Tpm1^2-0.0001024062*Tpm1+0.01895682)/
    (-0.003284948*Tpm1^2+1.687644*Tpm1+785.6677);
  Re=2*m*Di/(1000*pi*Di^2*visc）；
  Pr=visc/alfa;
  if (Re>2300)
    friction=(0.79*log(Re)-1.64)^-2;
    Nulong=(friction/8)*(Re-1000)*Pr/(1+12.7*sqrt(friction/8)*(Pr^(2/3)-1));
    Nu=Nulong*(1+(Di/ltube)^0.7);
```

```
    else
      Nu=4.4+0.00172*(Re*Pr*Di/ltube)^1.66/(1+0.00281*(Re*Pr*Di/ltube)^1.29);
    end
    thcond=-0.00000981358*Tpm1^2+0.007536807*Tpm1-0.7674181;
    hfi=Nu*thcond/Di;
    e=0.43*(1-100/Tpm1);
    Ut=(N/(C/Tpm1*((Tpm1-T)/(N+ef))^e+1/hw)^-1+(sb*(Tpm1+T)*
        (Tpm1^2+T^2))/((ep+0.00591*N*hw)^-1+(2*N+ef-1+0.133*ep)/eg-N));
    Qt=Ac*Ut*(Tpm1-T);
    Qb=kb/Lb*Ac*(Tpm1-T);
    Qe=ke/Le*Ae*(Tpm1-T);
    QL=Qt+Qb+Qe;
    UL=QL/(Ac*(Tpm1-T));
    UL2=UL*Ac/Ap;
    mi=(UL2/(kapa*delta))^0.5;
    F=tanh(mi*(W-D)/2)/(mi*(W-D)/2);
    F1=(1/UL2)/(W*(1/(UL2*(D+(W-D)*F))+1/Cb+1/(pi*Di*hfi)));
    FR=m*Cp/(Ap*UL2)*(1-exp(-Ap*UL2*F1/(m*Cp)));
    Qu=Ap*(S-UL2*(Tpm1-T));
    Tpm2=Tin+Qu/(Ap*FR*UL2)*(1-FR);
  end
  Tpm(i)=Tpm(i)+Tpm2;
  Quse=Ap*FR*(S-UL2*(Tin-T));
  F2=FR/F1;   %collector flow factor F''
  eff(i)=Quse/(Ac*(Ib+Id));
  x(i)=(Tin-T)/(Ib+Id);
  Tfm(i)=Tin+Quse/(Ap*FR*UL2)*(1-F2);
  Tin=Tin+0.1;
```

```
end
alpha2=(eff(1)-eff(700))/x(700);   %parameter α of collector equation
beta2=eff(1);    %parameter β of collector equation
plot(x,eff);
```

Bibliography

1. Philibert C. The present and future use of solar thermal energy as a primary source of energy; International Energy Agency; 2008.
2. Butti K., Perlin J. A Golden Thread: 2500 Years of Solar Architecture and Technology; Chesire Books; 2004.
3. http://www.ises.org (International Solar Energy Society)
4. Honsberg C., Bowden S. PVCDROM; pveducation.org.
5. http://commons.wikimedia.org/wiki/File:Hukseflux_Pyranometer_SR03.jpg#file
6. http://www.soldata.dk/products.htm
7. Weiss W., Mauthner F. Solar Heat Worldwide: Markets and Contribution to the Energy Supply 2009; IEA Solar Heating & Cooling Programme; 2011.
8. Brechlin U. Worldwide capacity of solar thermal energy greatly underestimated; European Solar Thermal Industry Federation; 2004.
9. http://www.ebhe.gr/library/Sun_In_Action2_Vol1.pdf
10. Kalogirou S. Solar energy engineering: processes and systems; London: Elsevier; 2009.
11. http://www.indiamart.com/ssae-ltd/services.html
12. http://solarsmartliving.com/hot_water/how_it_works.asp
13. http://www.longislandsolarenergysystems.com/longislandsolarhotwatertechnol ogy.htm
14. http://www.jgheating.co.uk/gasshop/index.php?target=pages&page_id=solar_panels_installations
15. Bedi E., CANCEE, Falk H. Solar Collectors; energysavingnow.com; 2000.
16. http://solar-collector.net/?p=257
17. http://en.wikipedia.org/wiki/Solar_thermal_collector
18. http://www.hitemp.co.za/solargeyser.htm
19. http://www.builditsolar.com/Projects/SpaceHeating/Glazing.htm

20. http://wn.com/jcanivan

21. Tsilingiridis G., Martinopoulos G. Thirty years of domestic solar hot water systems use in Greece – energy and environmental benefits – future perspectives; Elsevier; 2009.

22. Duffie J. A., Beckman W. A. Solar Engineering of Thermal Processes, 2nd Edition; New York: John Wiley & Sons; 1991.

23. Twidell J., Weir T. Renewable Energy Resources, 2nd Edition; Taylor & Francis; 2006.

24. Koo J. M., Development of a flat plate solar collector design program; University of Wisconsin-Madison; 1999.